

The calcium sensor synaptotagmin 7 is required for synaptic facilitation

Skyler L. Jackman¹, Josef Turecek¹, Justine E. Belinsky¹ & Wade G. Regehr¹

It has been known for more than 70 years that synaptic strength is dynamically regulated in a use-dependent manner¹. At synapses with a low initial release probability, closely spaced presynaptic action potentials can result in facilitation, a short-term form of enhancement in which each subsequent action potential evokes greater neurotransmitter release². Facilitation can enhance neurotransmitter release considerably and can profoundly influence information transfer across synapses³, but the underlying mechanism remains a mystery. One proposed mechanism is that a specialized calcium sensor for facilitation transiently increases the probability of release^{2,4}, and this sensor is distinct from the fast sensors that mediate rapid neurotransmitter release. Yet such a sensor has never been identified, and its very existence has been disputed^{5,6}. Here we show that synaptotagmin 7 (Syt7) is a calcium sensor that is required for facilitation at several central synapses. In Syt7-knockout mice, facilitation is eliminated even though the initial probability of release and the presynaptic residual calcium signals are unaltered. Expression of wild-type Syt7 in presynaptic neurons restored facilitation, whereas expression of a mutated Syt7 with a calcium-insensitive C2A domain did not. By revealing the role of Syt7 in synaptic facilitation, these results resolve a longstanding debate about a widespread form of short-term plasticity, and will enable future studies that may lead to a deeper understanding of the functional importance of facilitation.

Several mechanisms for facilitation have been proposed (Extended Data Fig. 1). In the ‘buffer saturation’ model, high concentrations of presynaptic Ca^{2+} buffer capture incoming Ca^{2+} before it binds to the rapid synaptotagmin isoforms (1, 2 and 9) that trigger vesicle fusion at most synapses⁷. If the Ca^{2+} buffer saturates during the first action potential, more Ca^{2+} reaches release sites during subsequent action potentials, producing facilitation^{6,8}. Yet many facilitating synapses lack sufficient presynaptic Ca^{2+} buffer to account for this form of facilitation⁹. Another theory suggests that a specialized Ca^{2+} sensor responds to the smaller, longer-lasting Ca^{2+} signals between action potentials⁴. In one scenario, this sensor modulates Ca^{2+} channels to produce use-dependent increases in Ca^{2+} influx¹⁰. Several candidate proteins have been proposed to act in this manner^{11,12}, but increased Ca^{2+} influx cannot account for facilitation at most synapses¹³. Alternatively, an unidentified Ca^{2+} sensor could mediate facilitation by directly increasing the probability of release (p).

Syt7 is located presynaptically, and binds Ca^{2+} with high affinity and slow kinetics^{14–16}, making it a promising candidate sensor for the modest increases in residual Ca^{2+} that mediate facilitation. Previous studies suggest that Syt7 contributes to a slow phase of transmission known as asynchronous release^{17,18}, and to Ca^{2+} -dependent recovery from depression¹⁹, but the role of Syt7 in facilitation was not examined because these studies used synapses with prominent depression that obscures facilitation. We therefore examined synaptic transmission at four facilitating synapses: Schaffer collateral synapses between hippocampal CA3 and CA1 pyramidal cells⁹ (Fig. 1a), thalamocortical synapses between layer 6 cortical pyramidal cells and thalamic relay

cells²⁰ (Fig. 1b), mossy fibre synapses between dentate granule and CA3 cells⁹ (Fig. 1c), and perforant path synapses between layer II and III cells of the entorhinal cortex and dentate granule cells²¹ (Fig. 1d). Immunohistochemistry shows that Syt7 is present in regions where these synapses are located (Extended Data Figs 2 and 3). Facilitation is often assessed using pairs of closely spaced stimuli. In slices from wild-type mice, paired-pulse facilitation resulted in ~2-fold enhancement of neurotransmitter release lasting several hundred milliseconds (Fig. 1a–d, black traces). In Syt7-knockout mice, paired-pulse facilitation was eliminated (Fig. 1a–d, red traces). Sustained high frequency activation produces up to tenfold enhancement in wild-type animals, but facilitation is eliminated in knockouts at all synapses except for mossy fibre synapses, where the remaining enhancement is consistent with use-dependent spike broadening that occurs at this synapse²² (Fig. 1e–h and Extended Data Fig. 4).

The loss of facilitation in Syt7 knockouts cannot be accounted for by slowed recovery from depression reported with Syt7 deletion¹⁹, because recovery from depression is too slow to influence rapid facilitation strongly, nor can it produce the large increase in release associated with facilitation. There are several possible explanations for the loss of facilitation in knockouts: (1) the presynaptic Ca^{2+} signal that induces facilitation could be altered, (2) the probability of release (p) for synaptic vesicles could be increased, which by promoting vesicle depletion would indirectly reduce facilitation, or (3) the mechanism for facilitation could be disrupted directly. We assessed these possibilities at the CA3–CA1 synapse.

Action-potential-evoked increases in presynaptic Ca^{2+} consist of a large, brief localized Ca^{2+} signal that activates the low-affinity Ca^{2+} sensor synaptotagmin 1 to trigger neurotransmitter release²³, and a small residual Ca^{2+} signal (Ca_{res}) that persists for tens of milliseconds and has been implicated in facilitation². It is difficult to measure local Ca^{2+} signals that trigger release, but Ca_{res} is readily measured. We used a low-affinity Ca^{2+} indicator to measure the time course of Ca_{res} in CA3 presynaptic terminals, because facilitation can be attenuated by the accelerated decay of Ca_{res} (ref. 4). Ca_{res} decayed similarly in wild-type and Syt7-knockout animals (Fig. 2a), indicating that the loss of facilitation in knockout mice is not a consequence of accelerated Ca_{res} decay. We also used Ca_{res} as a measure of $\text{Ca}_{\text{influx}}$ to determine whether there are use-dependent changes in Ca^{2+} entry. However, each of two closely spaced stimuli evoked the same incremental increase in Ca_{res} in both wild types and knockouts (Fig. 2b), indicating that use-dependent changes in total $\text{Ca}_{\text{influx}}$ cannot account for facilitation. This suggests that if changes in $\text{Ca}_{\text{influx}}$ contribute to facilitation at this synapse, they must be restricted to the small subset of presynaptic calcium channels that evoke neurotransmitter release. We repeated the experiment using a high-affinity Ca^{2+} indicator, in which the degree of saturation during paired stimuli can be used to measure the magnitude of Ca_{res} evoked by the first stimulus (see Methods). We conclude that $\text{Ca}_{\text{influx}}$ evoked by the first stimulus is the same in wild-type and knockout animals (Fig. 2c).

We further explored the role of Ca^{2+} in facilitation by examining the Ca^{2+} -dependence of excitatory postsynaptic currents (EPSCs)

¹Department of Neurobiology, Harvard Medical School, 220 Longwood Avenue, Boston, Massachusetts 02115, USA.

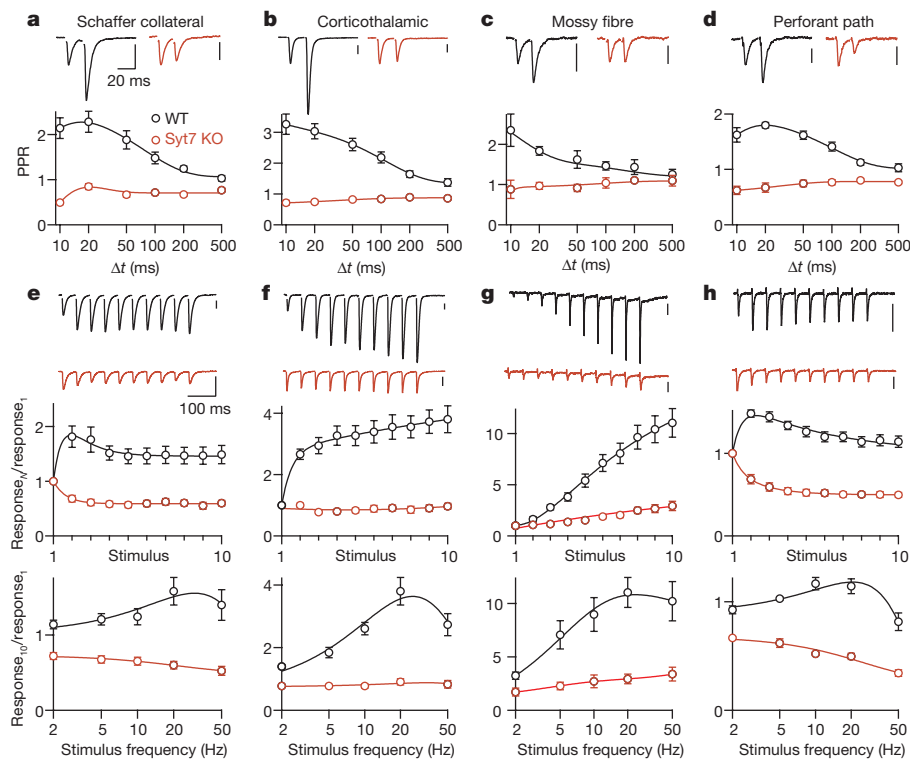


Figure 1 | Facilitation is absent in Syt7 knockout mice.

a–d, Representative traces (top) and average paired-pulse ratio (PPR) at different interstimulus intervals (Δt) (bottom) recorded in slices prepared from wild-type (WT; black) and Syt7-knockout (KO; red) animals. Postsynaptic responses were recorded using whole-cell voltage clamp from hippocampal CA1 pyramidal cells (**a**), and thalamic relay cells (**b**). fEPSPs were recorded from hippocampal-mossy-fibre to CA3 synapses (**c**), and lateral-perforant-path synapses in the dentate gyrus (**d**).

and facilitation. Raising extracellular Ca^{2+} leads to a steep increase in EPSC amplitude (Fig. 2d) but a decrease in facilitation (Fig. 2e, black traces), even though high extracellular Ca^{2+} should increase the Ca_{res} available to evoke facilitation. This paradox is resolved by realizing that increased Ca^{2+} influx increases p , which depletes presynaptic vesicles, saturates release and limits the extent of facilitation. The Ca^{2+} -dependence of EPSC amplitudes was unaffected in knockout animals (Fig. 2d), but facilitation was absent for all values of external Ca^{2+} (Fig. 2e, f). Meanwhile, there was no difference in basal release properties measured by the rate of spontaneous EPSCs (Extended Data Fig. 5). These findings suggest that the loss of facilitation in knockouts is not a consequence of higher initial p , because facilitation was absent even when the initial p was strongly attenuated by reducing external Ca^{2+} .

To test further whether initial p is increased in Syt7 knockouts, we measured how field excitatory postsynaptic potentials (fEPSPs) scaled with stimulus intensity²⁴ (Fig. 3a). The slope of the fEPSP versus presynaptic volley gives a relative measure of p (see Methods), which was unchanged in knockouts (Fig. 3b). Moreover, the fEPSP to presynaptic volley ratio changed steeply with extracellular Ca^{2+} , showing that this method is sensitive to p (Fig. 3c, d). We also assessed p using pharmacological blockade of synaptically activated NMDARs (*N*-methyl-D-aspartate receptors) by the use-dependent blocker MK801 (ref. 25; Fig. 3e–g). This approach is widely used to detect changes in p : an increase in p leads to more glutamate release, and more activation and rapid blockade of NMDARs, while a decrease in p leads to a slower blockade (Extended Data Fig. 6). The rate of blockade of NMDAR-mediated fEPSPs (NMDAR-fEPSPs) was unaffected by Syt7 deletion (Fig. 3e), indicating similar initial p . However, when we evoked NMDAR-fEPSPs with trains of three stimuli²⁵, amplitudes decayed more rapidly in wild types (Fig. 3f, g), suggesting that Syt7 is required to increase p for the second and third stimuli. Thus, initial p and presynaptic Ca^{2+}

Vertical scale bars, 100 pA (**a, b**) and 100 μV (**c, d**). **e–h**, Synaptic responses to 20-Hz trains from the same preparations as **a–d** (top), normalized amplitudes during 20-Hz trains (middle), and normalized responses to the tenth stimulus as a function of stimulus frequency (bottom). Peak PPR was significantly different for wild-type and Syt7-knockout mice at all synapses, as was response₁₀/response₁ for 5–50-Hz trains ($P < 0.01$, Student's *t*-test). Data represent mean \pm s.e.m. Number of experiments is shown in Extended Data Table 1.

signalling are unaffected by Syt7 deletion, but knockouts lack the use-dependent increase in p that underlies facilitation. This suggests that the mechanism underlying facilitation is directly impaired by Syt7 deletion.

Syt7 is implicated in neuroendocrine release¹⁶, insulin secretion²⁶ and exocytosis of lysosomes²⁷, which could all indirectly influence synaptic transmission in global Syt7 knockouts. Therefore, to determine whether Syt7 controls facilitation by acting in presynaptic neurons in a cell-autonomous manner, we tested whether viral expression of Syt7 in CA3 pyramidal cells of Syt7 knockouts rescued facilitation. This approach is complicated by our inability to virally transduce all CA3 pyramidal cells, which prohibits the use of extracellular stimulation that would activate some presynaptic cells that express Syt7 and others that do not. We overcame this problem with an adeno-associated virus (AAV) that drove bicistronic expression of both channelrhodopsin-2 (ChR2) and Syt7, allowing optical stimulation of only those fibres expressing Syt7.

Using conditions we have previously shown allow facilitation to be studied with optogenetic stimulation (see Methods), we confirmed that when ChR2 alone was expressed, optical and electrical stimulation produced similar facilitation in wild types (Fig. 4a, e, f), and similar depression in knockouts (Fig. 4b, e, f). We next used a bicistronic vector to express both ChR2 and wild-type Syt7 in knockout animals. Light-evoked responses exhibited facilitation, whereas electrically evoked responses did not (Fig. 4c, e, f). This suggests that bicistronic expression of ChR2 along with a presynaptic protein of interest offers a powerful new approach to characterize the effect of gene manipulation on presynaptic function within intact neural circuits. When Syt7 was expressed in wild-type animals, the peak facilitation was unaffected (Fig. 4e, f and Extended Data Fig. 7a). Thus, expressing Syt7 in CA3 pyramidal cells rescued facilitation in a cell-autonomous manner, with facilitation restored only at synapses expressing Syt7 and ChR2.

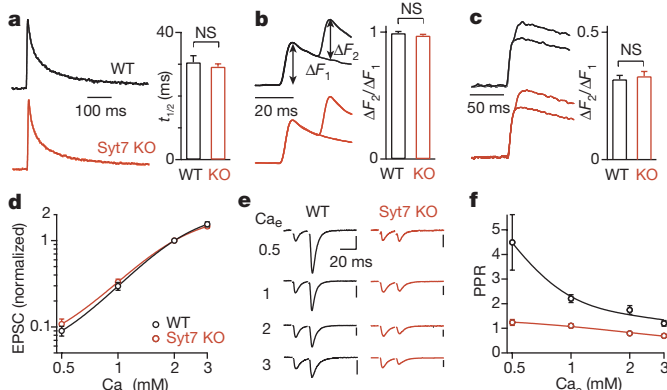


Figure 2 | Facilitation is altered in Syt7-knockout animals despite similar presynaptic Ca^{2+} signals. **a**, Presynaptic Ca_{res} evoked by a single stimulus recorded from Schaffer collateral fibres loaded with a low-affinity Ca^{2+} indicator (left), and Ca_{res} half-decay times (right). NS, not significant. **b**, Ca_{res} signals recorded with low-affinity indicator evoked by one or two stimuli (left). The ratio of the increase in Ca_{res} evoked by the first (ΔF_1) and second (ΔF_2) stimuli (right). **c**, Ca_{res} signals recorded with high-affinity indicator evoked by one or two stimuli. **d**, Average EPSC amplitudes for CA3–CA1 synapses recorded in different external Ca^{2+} (Ca_e) concentrations, normalized to the amplitude in 2 mM Ca_e . **e**, EPSCs recorded in different Ca_e . Vertical scale bars, 50, 100, 200 and 300 pA in 0.5, 1, 2 and 3 mM Ca_e , respectively. **f**, PPR for interstimulus interval of 20 ms recorded in different Ca_e . In 0.5 mM Ca^{2+} , the PPR in knockout (1.24 ± 0.12) was not significantly different from 1 ($P = 0.084$, Wilcoxon signed rank test). Data represent mean \pm s.e.m. Number of experiments is shown in Extended Data Table 2.

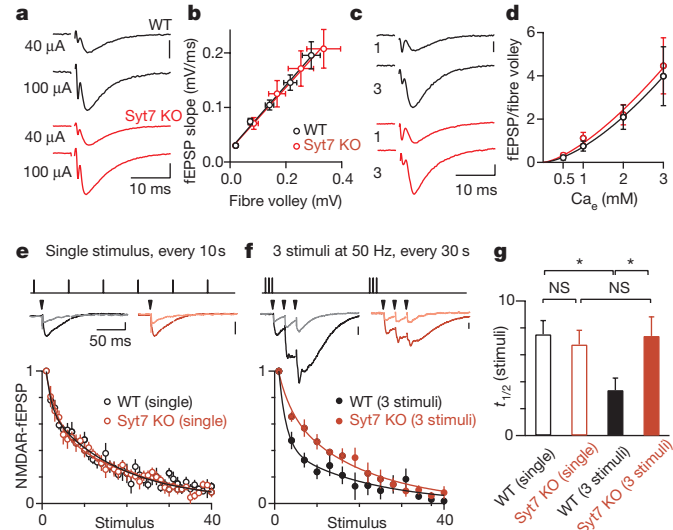


Figure 3 | Change in the initial probability of release does not underlie the absence of facilitation in Syt7-knockout mice. **a**, Extracellular recordings of presynaptic fibre volley and fEPSP evoked by the indicated stimulus intensities. Scale bar, 200 μV . **b**, fEPSP slope plotted against fibre volley amplitude, for 20–100 μA stimulation. **c**, fEPSPs recorded in 1 and 3 mM Ca_e . Scale bar, 100 μV . **d**, Average ratio of the fEPSP to the fibre volley in different Ca_e . **e**, Top, initial release probability was measured by stimulating Schaffer collaterals every 10 s while recording NMDAR-fEPSPs before and after MK801 bath application. Middle, traces averaged from 10 trials before (dark traces), and trials 10–15 after (light traces) MK801 application. Bottom, average NMDAR-fEPSP amplitudes evoked in the presence of MK801. **f**, Same as in **e** but with three stimuli at 50 Hz every 30 s. First response to trains is shown. **g**, Half-decay times of NMDAR-fEPSP amplitudes in the presence of MK801. * $P < 0.05$, one-way analysis of variance (ANOVA) with Tukey's post-hoc test. Data represent mean \pm s.e.m. Number of experiments shown in Extended Data Table 2.

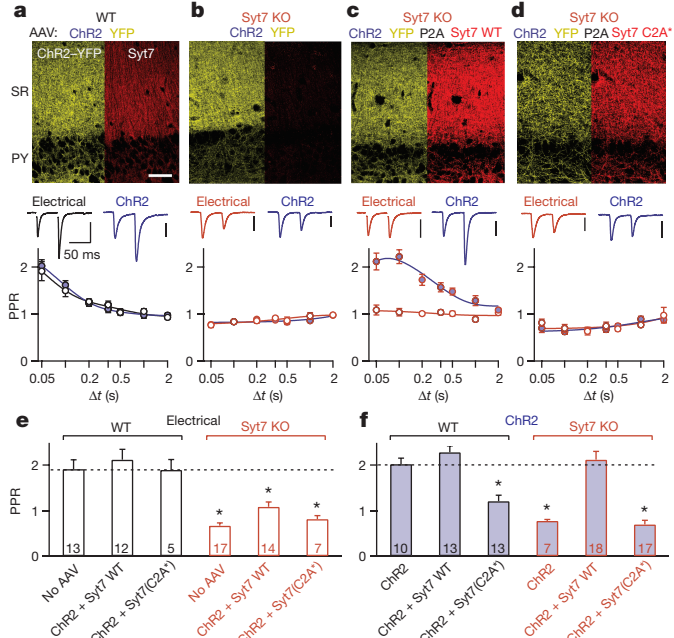


Figure 4 | Viral expression of Syt7 restores facilitation at Schaffer collateral synapses. **a–d**, Top, fluorescence images of yellow fluorescent protein (YFP)-tagged ChR2 and Syt7 immunostaining in the CA1 region after AAV injection into CA3 to express the indicated proteins in wild-type animals (**a**) or Syt7-KO animals (**b–d**). PY, stratum pyramidale; SR, stratum radiatum. Scale bar, 100 μm . Bottom, EPSCs and PPRs for responses evoked electrically (open symbols) and optically (blue symbols). In **a** and **b**, only ChR2-YFP was expressed; in **c**, both ChR2-YFP and wild-type Syt7 were expressed (separated by a porcine teschovirus-1 2A (P2A) cleavage peptide); and in **d**, ChR2-YFP and Ca^{2+} -insensitive Syt7(C2A*) were expressed. **e**, **f**, Summary of PPRs for 50-ms interstimulus interval. Asterisks denote significant difference from responses evoked electrically in uninjected wild-type animals (**e**), or optically in wild-type animals expressing ChR2 alone (**f**). * $P < 0.05$, one-way ANOVA with Tukey's post-hoc test. Data represent mean \pm s.e.m. Number of experiments is shown on bar graphs.

To determine whether Ca^{2+} binding by Syt7 is important for facilitation, we assessed whether facilitation is rescued by Syt7 with a mutated Ca^{2+} -insensitive C2A domain (Syt7(C2A*)). Previous studies established that Ca^{2+} binding to the C2A domain of Syt7 is required for Syt7 to mediate asynchronous release¹⁸. We found that Syt7(C2A*) did not rescue facilitation in knockouts (Fig. 4d–f). Moreover, in wild-type animals, Syt7(C2A*) expression strongly attenuated facilitation (Fig. 4e, f and Extended Data Fig. 7b), suggesting that Syt7(C2A*) competes with native Syt7 to suppress facilitation.

Our results indicate that facilitation requires Ca^{2+} binding to the C2A domain of Syt7, and also provide insight into the role of Syt7 in facilitation. We conclude that Syt7 does not produce facilitation by altering the amplitude and time course of Ca_{res} (Fig. 2), by increasing initial p (Fig. 3), by acting as a Ca^{2+} buffer (Extended Data Fig. 8), or through use-dependent increases in the total $\text{Ca}_{\text{influx}}$ (Extended Data Fig. 1b and Fig. 2). The observation that initial p is unaltered in Syt7 knockouts indicates that local $\text{Ca}_{\text{influx}}$ is unaffected for the first stimulus, but it is difficult to rule out the possibility that Syt7 mediates a use-dependent increase in $\text{Ca}_{\text{influx}}$ through the subset of channels that trigger vesicle fusion. There is, however, no evidence for Syt7 associating with or regulating calcium channels. By contrast, Syt7 is known to interact with Syt1 and can mediate vesicle fusion^{16–18}. The most parsimonious explanation is that Syt7 acts as the proposed specialized Ca^{2+} sensor to increase p during facilitation. Facilitated release exhibits rapid kinetics, suggesting that Syt7 somehow increases the probability of Syt1-dependent vesicle fusion. Whether this is through a direct interaction of Syt7 with a fast synaptotagmin isoform such as

Syt1 remains an open question. It is also unclear whether the recently described interaction between Syt7 and calmodulin that promotes vesicle replenishment¹⁹ is similarly required for facilitation. Finally, it is possible that at other synapses facilitation is mediated by additional specialized Ca^{2+} sensors, or involves other mechanisms. Further studies are needed to clarify these issues.

Based primarily on theoretical considerations, facilitation is thought to influence both information transfer and network dynamics profoundly. In the hippocampus, the high-pass filtering imposed by facilitating synapses may account for the burst firing in place cells that encode spatial information²⁸. In the auditory pathway, facilitation is proposed to counteract short-term depression to maintain linear transmission of rate-coded sound intensity²⁹. It has even been suggested that facilitation forms the basis of short-term memory, as facilitating recurrent connections within cortical networks could support the persistent activity states associated with working memory³⁰. In future studies, the selective elimination of Syt7 from specific cell types could allow the first direct tests of the effect of facilitation on neural circuits and behaviour.

Online Content Methods, along with any additional Extended Data display items and Source Data, are available in the online version of the paper; references unique to these sections appear only in the online paper.

Received 4 June; accepted 3 December 2015.

1. Feng, T. P. Studies on the neuromuscular junction. XVIII. The local potentials around n-m junctions induced by single and multiple volleys. *Chin. J. Physiol.* **15**, 367–404 (1940).
2. Zucker, R. S. & Regehr, W. G. Short-term synaptic plasticity. *Annu. Rev. Physiol.* **64**, 355–405 (2002).
3. Abbott, L. F. & Regehr, W. G. Synaptic computation. *Nature* **431**, 796–803 (2004).
4. Atluri, P. P. & Regehr, W. G. Determinants of the time course of facilitation at the granule cell to Purkinje cell synapse. *J. Neurosci.* **16**, 5661–5671 (1996).
5. Bertram, R., Sherman, A. & Stanley, E. F. Single-domain/bound calcium hypothesis of transmitter release and facilitation. *J. Neurophysiol.* **75**, 1919–1931 (1996).
6. Felmy, F., Neher, E. & Schneggenburger, R. Probing the intracellular calcium sensitivity of transmitter release during synaptic facilitation. *Neuron* **37**, 801–811 (2003).
7. Südhof, T. C. A molecular machine for neurotransmitter release: synaptotagmin and beyond. *Nature Med.* **19**, 1227–1231 (2013).
8. Matveev, V., Zucker, R. S. & Sherman, A. Facilitation through buffer saturation: Constraints on endogenous buffering properties. *Biophys. J.* **86**, 2691–2709 (2004).
9. Blatow, M., Caputi, A., Burnashev, N., Monyer, H. & Rozov, A. Ca^{2+} buffer saturation underlies paired pulse facilitation in calbindin-D28k-containing terminals. *Neuron* **38**, 79–88 (2003).
10. Mochida, S., Few, A. P., Scheuer, T. & Catterall, W. A. Regulation of presynaptic CaV2.1 channels by Ca^{2+} sensor proteins mediates short-term synaptic plasticity. *Neuron* **57**, 210–216 (2008).
11. Sippy, T., Cruz-Martin, A., Jeromin, A. & Schweizer, F. E. Acute changes in short-term plasticity at synapses with elevated levels of neuronal calcium sensor-1. *Nature Neurosci.* **6**, 1031–1038 (2003).
12. Tsujimoto, T., Jeromin, A., Saitoh, N., Roder, J. C. & Takahashi, T. Neuronal calcium sensor 1 and activity-dependent facilitation of P/Q-type calcium currents at presynaptic nerve terminals. *Science* **295**, 2276–2279 (2002).
13. Müller, M., Felmy, F. & Schneggenburger, R. A limited contribution of Ca^{2+} current facilitation to paired-pulse facilitation of transmitter release at the rat calyx of Held. *J. Physiol. (Lond.)* **586**, 5503–5520 (2008).
14. Hui, E. et al. Three distinct kinetic groupings of the synaptotagmin family: candidate sensors for rapid and delayed exocytosis. *Proc. Natl. Acad. Sci. USA* **102**, 5210–5214 (2005).
15. Li, C. et al. Ca^{2+} -dependent and -independent activities of neural and non-neural synaptotagmins. *Nature* **375**, 594–599 (1995).
16. Sugita, S. et al. Synaptotagmin VII as a plasma membrane Ca^{2+} sensor in exocytosis. *Neuron* **30**, 459–473 (2001).
17. Wen, H. et al. Distinct roles for two synaptotagmin isoforms in synchronous and asynchronous transmitter release at zebrafish neuromuscular junction. *Proc. Natl. Acad. Sci. USA* **107**, 13906–13911 (2010).
18. Bacaj, T. et al. Synaptotagmin-1 and synaptotagmin-7 trigger synchronous and asynchronous phases of neurotransmitter release. *Neuron* **80**, 947–959 (2013).
19. Liu, H. et al. Synaptotagmin 7 functions as a Ca^{2+} -sensor for synaptic vesicle replenishment. *eLife* **3**, e01524 (2014).
20. Deschênes, M. & Hu, B. Electrophysiology and pharmacology of the corticothalamic input to lateral thalamic nuclei: an intracellular study in the cat. *Eur. J. Neurosci.* **2**, 140–152 (1990).
21. Lømo, T. Potentiation of monosynaptic EPSPs in the perforant path-dentate granule cell synapse. *Exp. Brain Res.* **12**, 46–63 (1971).
22. Geiger, J. R. & Jonas, P. Dynamic control of presynaptic Ca^{2+} inflow by fast-inactivating K^+ channels in hippocampal mossy fiber boutons. *Neuron* **28**, 927–939 (2000).
23. Geppert, M. et al. Synaptotagmin I: a major Ca^{2+} sensor for transmitter release at a central synapse. *Cell* **79**, 717–727 (1994).
24. Dingledine, R. & Somjen, G. Calcium dependence of synaptic transmission in the hippocampal slice. *Brain Res.* **207**, 218–222 (1981).
25. Manabe, T. & Nicoll, R. A. Long-term potentiation: evidence against an increase in transmitter release probability in the CA1 region of the hippocampus. *Science* **265**, 1888–1892 (1994).
26. Gustavsson, N. et al. Impaired insulin secretion and glucose intolerance in synaptotagmin-7 null mutant mice. *Proc. Natl. Acad. Sci. USA* **105**, 3992–3997 (2008).
27. Martinez, I. et al. Synaptotagmin VII regulates Ca^{2+} -dependent exocytosis of lysosomes in fibroblasts. *J. Cell Biol.* **148**, 1141–1150 (2000).
28. Klyachko, V. A. & Stevens, C. F. Excitatory and feed-forward inhibitory hippocampal synapses work synergistically as an adaptive filter of natural spike trains. *PLoS Biol.* **4**, e207 (2006).
29. MacLeod, K. M., Horiuchi, T. K. & Carr, C. E. A role for short-term synaptic facilitation and depression in the processing of intensity information in the auditory brain stem. *J. Neurophysiol.* **97**, 2863–2874 (2007).
30. Mongillo, G., Barak, O. & Tsodyks, M. Synaptic theory of working memory. *Science* **319**, 1543–1546 (2008).

Acknowledgements We thank P. Kaeser and L. Bickford for help with producing AAVs, B. Sabatini and J. Levesque for help with plasmids, K. Ennis, M. Ocana and the Neurobiology Imaging Center for help with immunohistochemistry, B. Sabatini, P. Kaeser, D. Fioravante, C. Hull and L. Glickfeld for comments on the manuscript. This work was supported by grants from the National Institutes of Health (NIH; NS032405) and Nancy Lurie Marks Foundation to W.G.R., the Vision Core and NINDS P30 Core Center grant (NS072030) to the Neurobiology Imaging Center at Harvard Medical School, and a Nancy Lurie Marks Fellowship to S.L.J.

Author Contributions S.L.J., J.T. and W.G.R. designed experiments. J.E.B. performed stereotaxic surgeries, S.L.J. performed electrophysiology, and J.T. measured Ca^{2+} and performed immunohistochemistry. S.L.J. and J.T. produced AAVs and analysed experiments, and S.L.J. and W.G.R. wrote the manuscript.

Author Information Reprints and permissions information is available at www.nature.com/reprints. The authors declare no competing financial interests. Readers are welcome to comment on the online version of the paper. Correspondence and requests for materials should be addressed to W.G.R. (wade_regehr@hms.harvard.edu).

METHODS

Animals and viruses. All mice were handled in accordance with NIH guidelines and protocols approved by Harvard Medical School. Syt7 knockout mice³¹ (Jackson Laboratory) and wild-type littermates of either sex were used. Statistical tests were not used to predetermine sample size. Blinding and randomization were not performed. AAV2/9-hSyn-hChR2(H134R)-EYFP and its pAAV backbone (Addgene 26973) were obtained from the University of Pennsylvania Vector Core. Complementary DNA encoding the rat Syt7 wild-type α isoform and C2A* mutant (D225A, D227A and D233A)¹⁸ were provided by T. Bacaj and T. Sudhof. For rescue experiments involving Syt7 with mutated Ca^{2+} binding domains, we used the mutated C2A* version instead of the C2A*C2B* double mutant, as mutation of both C2 domains leads to lower levels of expression. The P2A cleavage sequence³² and Syt7 were inserted after the ChR2 carboxy terminus in the pAAV backbone (Genscript). Plasmid-driven expression of ChR2-YFP and Syt7 was confirmed in HEK cells by Syt7 immunostaining and patch-clamp recording of ChR2 photocurrents. AAVs were produced and purified from HEK cells as previously described³³.

Stereotaxic surgeries were performed as described³⁴. Postnatal day (P) 18–30 mice were anaesthetized with ketamine/xylazine/acepromazine (100/10/3 mg kg⁻¹) supplemented with 1–4% isoflurane. Viruses were injected through glass capillary needles using a syringe (Hamilton) mounted on a stereotaxic instrument (Kopf). Injection coordinates from lambda were 2.69 mm (rostro), 3 mm (lateral) and 2.8 mm (ventral). One microlitre of virus suspension was delivered at a rate of 0.1 $\mu\text{l min}^{-1}$ using a microsyringe pump (WPI; UMP3) and microsyringe pump controller (WPI; Micro4). The needle was slowly retracted 5–10 min after injection, and the scalp incision was closed with gluture. Post-injection analgesic (buprenorphine, 0.05 mg kg⁻¹) was administered subcutaneously for 48 h.

Acute slice preparation. P30–P60 animals were euthanized under isoflurane anaesthesia, 14–30 days after AAV injection. Brains were removed and placed in ice-cold solution containing (in mM): 234 sucrose, 25 NaHCO₃, 11 glucose, 7 MgCl₂, 2.5 KCl, 1.25 NaH₂PO₄ and 0.5 CaCl₂. Then, 270- μm -thick transverse slices (hippocampal recordings) or 250- μm -thick sagittal slices (thalamic recordings) were prepared on a vibratome (Leica, VT1000s), and a cut was made between CA3 and CA1 to prevent recurrent excitation. Slices were transferred for 30 min to 32 °C artificial cerebrospinal solution (ACSF) containing (in mM): 125 NaCl, 26 NaHCO₃, 25 glucose, 2.5 KCl, 2 CaCl₂, 1.25 NaH₂PO₄ and 1 MgCl₂, adjusted to 315 mOsm, and allowed to equilibrate to room temperature for >30 min. Experiments were performed at 33 ± 1 °C with flow rates of 2 ml min⁻¹.

Electrophysiology. For ChR2 stimulation, 160 mW mm⁻² laser pulses (0.2–0.5 ms) from a 100-mW 473 nm laser (OptoEngine, MBL-III) were focused through the $\times 60$ objective of the microscope (Olympus, BX51WI) to produce a 80- μm diameter spot over the stratum radiatum, >500 μm from the recorded cell to avoid activating ChR2 in presynaptic boutons, which can artificially raise the probability of release and obscure facilitation³⁴. Extracellular stimulation was performed with a stimulus isolation unit (WPI, A360) using glass monopolar electrodes (0.5–1 M Ω) filled with ACSF. Stimulus electrodes were positioned ~500 μm from the recording electrode in the stratum radiatum (Schaffer collaterals), the internal capsule (corticothalamic), the hilus adjacent to the dentate granule cell layer (mossy fibres), and the outer molecular layer (lateral perforant path). To ensure that mossy fibre responses were not contaminated by associational/commissural inputs the metabotropic glutamate receptor agonist DCG-IV (1 μM) was applied at the end of experiments to block mossy fibre responses selectively³⁵. Data were included only if responses were reduced by more than 80% (average reduction was 88 ± 1% in wild-type and 90 ± 2% in Syt7-knockout mice), and the amplitude of mossy fibre responses was measured after subtracting the response remaining in the presence of DCG-IV. Stimulus trials were repeated at 0.1 Hz (0.033 Hz at mossy fibres to avoid potentiation), and artefacts were deleted for display. Recordings were acquired using an amplifier (Axon Instruments, Multiclamp 700B) controlled by custom software written in IgorPro (provided by Matthew Xu-Friedman, SUNY Buffalo), and low-pass filtered at 2 kHz. Whole-cell recordings were obtained using borosilicate patch pipettes (2–5 M Ω) pulled with a horizontal puller (Sutter P-97). The internal recording solution contained (in mM): 150 Cs-gluconate, 3 KCl, 10 HEPES, 0.5 EGTA, 3 MgATP, 0.5 NaGTP, 5 phosphocreatine-Tris and 5 phosphocreatine-Na; pH 7.2. Cells were held at −70 mV, and series resistance was monitored during recordings. fEPSPs were recorded in current-clamp mode with ACSF-filled patch pipettes (0.5–1 M Ω). Inhibition was blocked with picrotoxin (50 μM), and during fEPSP recordings, CPP (2 μM) and CGP (3 μM) was added to the bath. Approximately 4–10 trials were conducted for each stimulus frequency, and recordings were averaged over trials. Data in all figures represent the mean ± s.e.m. Average responses are displayed with double exponential or

polynomial curves fit in IgorPro. Unless stated otherwise, statistical significance was assessed by unpaired two-tailed Student's *t*-test, or one-way ANOVA followed by Tukey's post-hoc test.

Probability of release. To record NMDAR-EPSCs, cells were voltage clamped at +40 mV, and the internal solution contained (in mM): 85 Cs-methanesulfonate, 4 NaCl, 10 HEPES, 0.2 EGTA, 30 BAPTA, 2 MgATP, 0.4 NaGTP, 10 phosphocreatine-Na, 25 TEA, 5 QX-314; pH 7.3. For recording NMDAR-fEPSPs, Mg²⁺ was excluded from ACSF to relieve Mg²⁺ block of NMDA receptors. Picrotoxin (100 μM) and NBQX (5 μM) were added to the bath, and stimulation was conducted at 0.1 Hz (unless otherwise indicated) for 5 min to obtain a baseline response. Stimulation was halted for 10 min while (+)-MK801 (40 μM) was added and allowed to equilibrate. For experiments involving fEPSPs versus presynaptic volley, the postsynaptic response was measured by the slope of the fEPSP, while the amplitude of the presynaptic volley was used to determine the number of activated fibres. If *p* increases, the same number of activated presynaptic fibres will produce a larger fEPSP. The ratio between fEPSP and volley was determined by line fits to the linear regime of the input–output curve of individual experiments (20–80 μA stimuli).

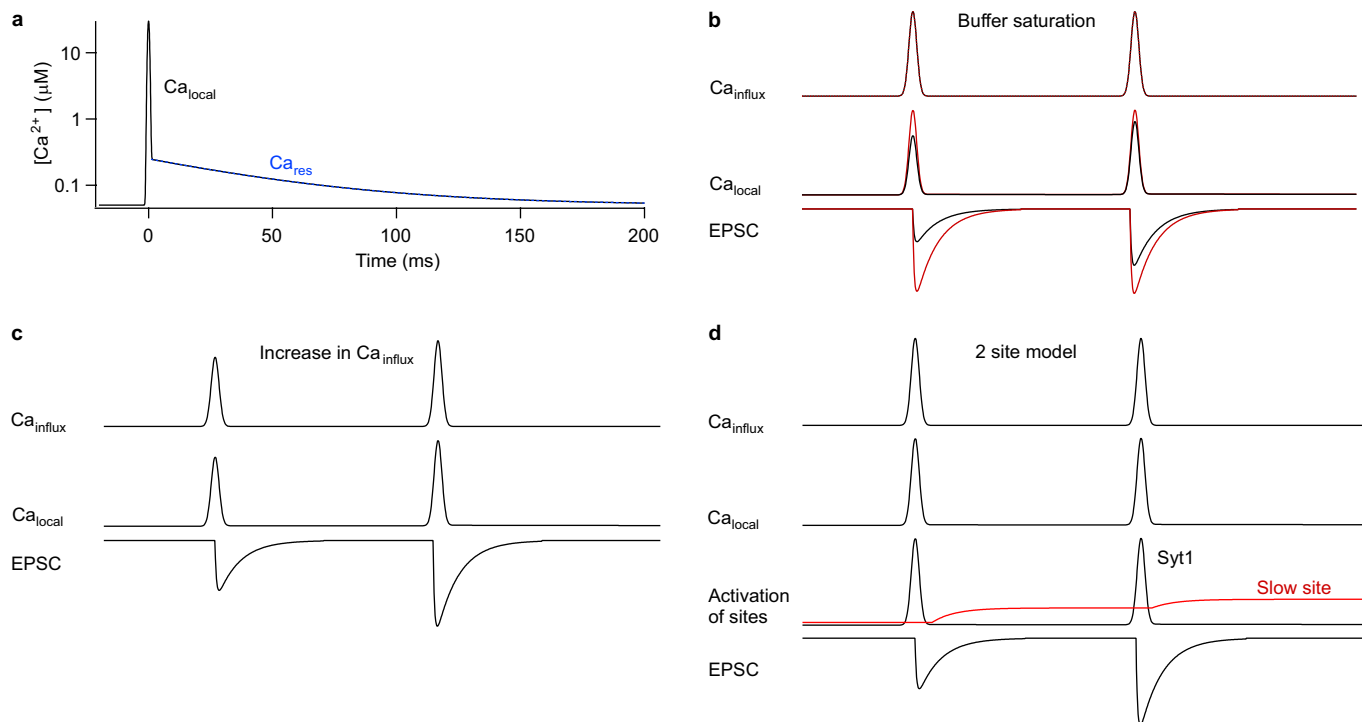
The study of probability of release is complicated because many people use *p* to refer to the probability of release of a vesicle (*p_v*) and others refer to probability of release from an active zone (*p_{synapse}*) that contains *N* vesicles in its readily releasable pool. Thus, an increase in the size of the readily releasable pool for an active zone can increase *p_{synapse}* even if *p_v* is unaltered. Although MK801 blockade²⁵ and fEPSPs versus presynaptic volley²⁴ are both widely used methods to detect changes in the probability of release, for both approaches it is conceivable (although unlikely) that increases in *p_v* could be obscured by a perfectly balanced decrease in the readily releasable pool size. However, the relationship between EPSC amplitude and extracellular Ca²⁺ is similar in wild-type and Syt7-knockout animals. This suggests there is no increase in *p_v*, which would cause this curve to saturate at lower values of Ca_e for Syt7-knockout animals. Moreover, the large differences in facilitation in wild-type and Syt7-knockout animals were even more pronounced when the probability of release was reduced tenfold by lowering Ca_e from 2 mM to 0.5 mM, which is incompatible with an increase in *p_v* obscuring facilitation by depleting vesicles.

Ca²⁺ measurements. Ca²⁺ was measured as described previously⁴. In brief, CA3 fibres were labelled for 3 min using an ACSF-filled pipette containing either magnesium green AM or fura-2 AM (240 μM) and 1% fast green, placed into the border of the CA3–CA1 field. A vacuum pipette placed above the loading site removed excess indicator. Slices were incubated for at least 1 h and imaging was performed in stratum radiatum of CA1 at least 500 μm from the injection site using a 60 \times objective and custom-built photodiode. Excitation was achieved using a tungsten (magnesium green) or xenon (fura-2) lamp. Schaffer collaterals were stimulated using a glass electrode placed at least 300 μm from the imaging site. To prevent recurrent excitation, experiments were performed in the presence of NBQX (10 μM), CPP (2 μM) and picrotoxin (50 μM).

Magnesium green is a low-affinity calcium indicator³⁶ (*K_D* = 7 μM) that provides an approximately linear measure of Ca_{res} (ref. 37). As such it is well suited to measuring the time course of presynaptic Ca_{res} (Fig. 2a) and detecting changes in Ca_{influx} during successive stimulations (Fig. 2b). However, with the bulk loading approach the size of the fluorescence change is proportional to the number of stimulated fibres, so the absolute Ca_{res} signal is not readily quantified with magnesium green. By contrast, fura-2 has a high affinity for calcium^{38,39} (*K_D* = 131 nM) so it provides a saturating sublinear response to increases in Ca_{res} (refs 40–42). This can be used to test for changes in the absolute size of Ca_{influx} because a change in the Ca_{influx} per stimulus would change the ratio between the fluorescence change produced by the first and second stimuli.

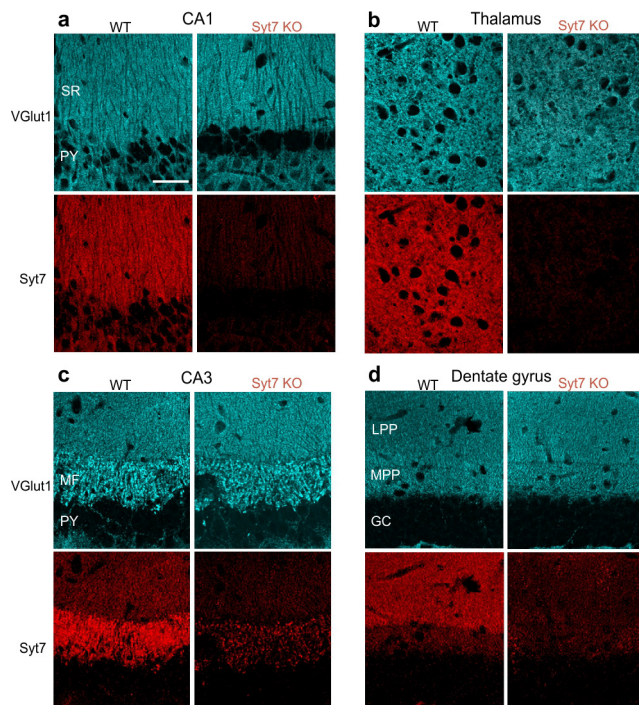
Immunohistochemistry. Two to four weeks after AAV injection, mice were anaesthetized with ketamine and transcardially perfused with 4% paraformaldehyde (PFA) in PBS. The brain was removed and post-fixed for 24 h. Slices (50 μm thick) were permeabilized (PBS plus 0.4% Triton X-100) for 30 min and then prepared in blocking solution (PBS plus 0.2% Triton X-100 and 2% normal goat serum; PBST) for 30 min at room temperature. Slices were incubated overnight at 4 °C in PBST with primary antibodies (anti-Syt7 (Synaptic Systems, 105173), 1 $\mu\text{g ml}^{-1}$; 1:200, targeting amino acids 46–133 of Syt7 α , anti-vGlut1 (Synaptic Systems, 135304), 1 $\mu\text{g ml}^{-1}$; 1:500, and anti-calbindin-D28k (Sigma Aldrich, C9848), 1 $\mu\text{g ml}^{-1}$; 1:500), followed by incubation with secondary antibodies in PBST for 2 h at room temperature. For both wild-type and Syt7-knockout mice, images from each brain region were acquired on a laser scanning confocal (Olympus, FluorView1200) using the same laser/microscope settings and processed in ImageJ identically.

31. Chakrabarti, S. *et al.* Impaired membrane resealing and autoimmune myositis in synaptotagmin VII-deficient mice. *J. Cell Biol.* **162**, 543–549 (2003).
32. Kim, J. H. *et al.* High cleavage efficiency of a 2A peptide derived from porcine teschovirus-1 in human cell lines, zebrafish and mice. *PLoS ONE* **6**, e18556 (2011).
33. Zolotukhin, S. *et al.* Recombinant adeno-associated virus purification using novel methods improves infectious titer and yield. *Gene Ther.* **6**, 973–985 (1999).
34. Jackman, S. L., Beneduce, B. M., Drew, I. R. & Regehr, W. G. Achieving high-frequency optical control of synaptic transmission. *J. Neurosci.* **34**, 7704–7714 (2014).
35. Kamiya, H., Shinozaki, H. & Yamamoto, C. Activation of metabotropic glutamate receptor type 2/3 suppresses transmission at rat hippocampal mossy fibre synapses. *J. Physiol. (Lond.)* **493**, 447–455 (1996).
36. Zhao, M., Hollingworth, S. & Baylor, S. M. Properties of tri- and tetracarboxylate Ca^{2+} indicators in frog skeletal muscle fibers. *Biophys. J.* **70**, 896–916 (1996).
37. Kreitzer, A. C. & Regehr, W. G. Modulation of transmission during trains at a cerebellar synapse. *J. Neurosci.* **20**, 1348–1357 (2000).
38. Brenowitz, S. D. & Regehr, W. G. Calcium dependence of retrograde inhibition by endocannabinoids at synapses onto Purkinje cells. *J. Neurosci.* **23**, 6373–6384 (2003).
39. Grynkiewicz, G., Poenie, M. & Tsien, R. Y. A new generation of Ca^{2+} indicators with greatly improved fluorescence properties. *J. Biol. Chem.* **260**, 3440–3450 (1985).
40. Sabatini, B. L. & Regehr, W. G. Detecting changes in calcium influx which contribute to synaptic modulation in mammalian brain slice. *Neuropharmacology* **34**, 1453–1467 (1995).
41. Maravall, M., Mainen, Z. F., Sabatini, B. L. & Svoboda, K. Estimating intracellular calcium concentrations and buffering without wavelength ratioing. *Biophys. J.* **78**, 2655–2667 (2000).
42. Sabatini, B. L. & Svoboda, K. Analysis of calcium channels in single spines using optical fluctuation analysis. *Nature* **408**, 589–593 (2000).
43. Regehr, W. G. Short-term presynaptic plasticity. *Cold Spring Harb. Perspect. Biol.* **4**, a005702 (2012).
44. Kaeser, P. S. & Regehr, W. G. Molecular mechanisms for synchronous, asynchronous, and spontaneous neurotransmitter release. *Annu. Rev. Physiol.* **76**, 333–363 (2014).
45. Kamiya, H. & Zucker, R. S. Residual Ca^{2+} and short-term synaptic plasticity. *Nature* **371**, 603–606 (1994).
46. Celio, M. R. Calbindin D-28k and parvalbumin in the rat nervous system. *Neuroscience* **35**, 375–475 (1990).

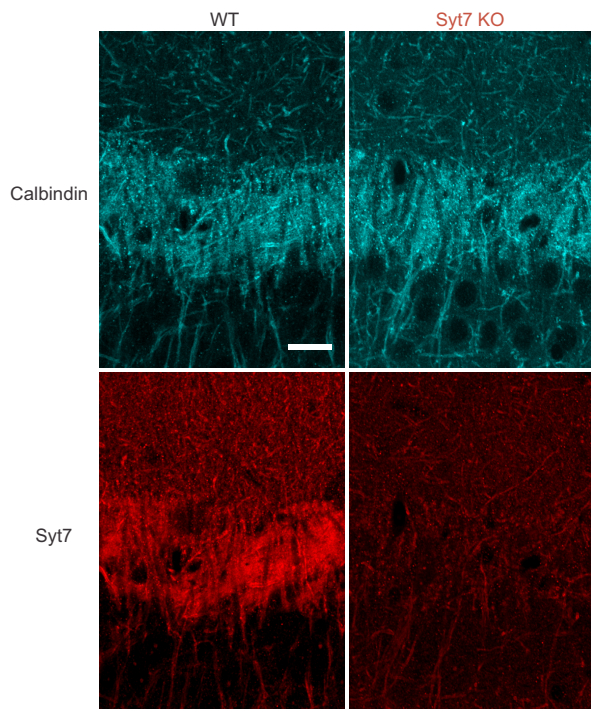

Extended Data Figure 1 | Possible mechanisms for synaptic facilitation.

a–d, It is established that calcium has an important role in synaptic facilitation, and several mechanisms have been proposed that involve different aspects of calcium signalling². Here we discuss the calcium signals that evoke rapid vesicle fusion, and also those thought to be involved in facilitation (**a**), and three mechanisms of facilitation are presented schematically⁴³ (**b–d**). **a**, To understand the mechanisms that have been proposed to account for facilitation, it is important to appreciate different aspects of presynaptic calcium signalling. Calcium signals are complex, but can be approximated by two components. An action potential opens calcium channels for less than a millisecond, and near open channels the calcium levels reach tens of micromolar. Release sites near calcium channels experience high local calcium levels (Ca_{local}) that are highly dependent on the distance from open calcium channels. Ca_{local} can be reduced by high concentrations of fast calcium buffers that rapidly bind calcium. In addition, there is a residual calcium signal (Ca_{res}) that results from calcium equilibrating within presynaptic terminals, before calcium is gradually removed over tens to hundreds of milliseconds. The amplitude of Ca_{res} (and also total influx of Ca^{2+} , Ca_{influx}) is determined by all of the calcium channels that open, not only those that produce Ca_{local} that drives release, and after initial equilibration Ca_{res} is roughly uniform throughout the presynaptic bouton. It is generally accepted that fast synaptic transmission is produced by calcium binding to Syt1, Syt2 or Syt9, which have low-affinity binding sites, fast kinetics, and require the binding of multiple calcium ions^{7,44}. The time course of release follows the time course of calcium channel opening, but with a brief delay (<1 ms). Ca_{res} after a single stimulus is much smaller than Ca_{local} . Typical fluorescence-based approaches to measure calcium readily detect Ca_{res} ,

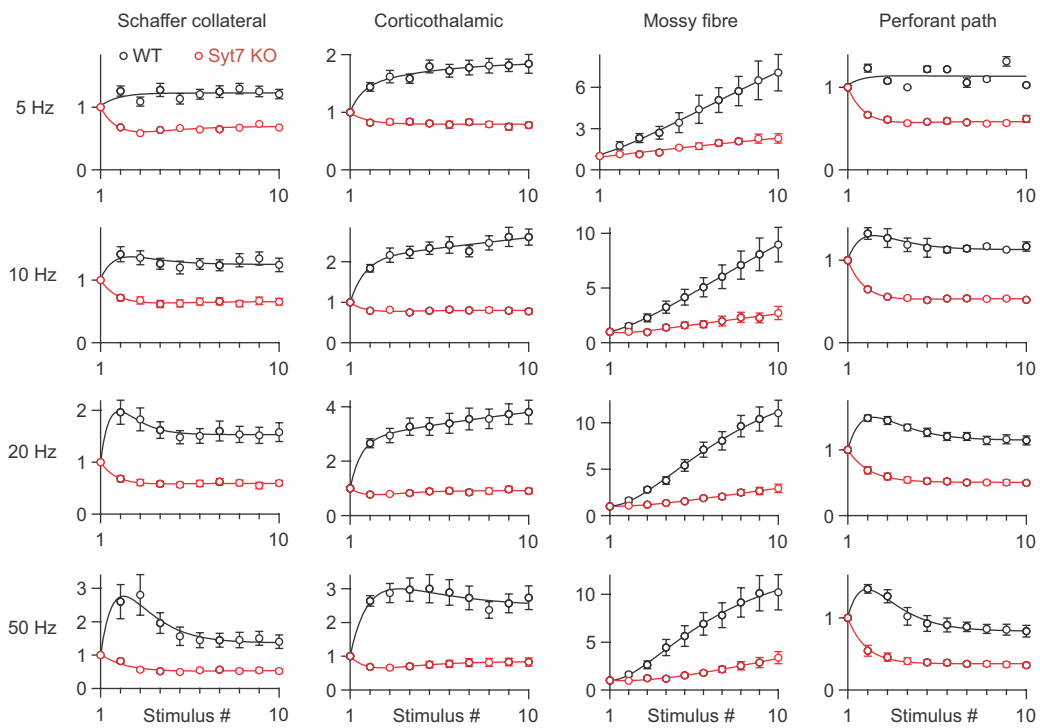
but are insensitive to Ca_{local} , which is too localized and short-lived to measure. Note the y axis is logarithmic to show both Ca_{local} and Ca_{res} in **a**, but not in **b–d**. **b**, For one mechanism of facilitation, a fast calcium buffer is present in presynaptic terminals that binds calcium and reduces Ca_{local} . Stimulation twice in rapid succession results in the same calcium influx for both stimuli. If there is no fast presynaptic buffer, the amplitudes of Ca_{local} and the EPSCs are the same for both stimuli (red traces). If a fast high-affinity buffer is present (black traces), it reduces the initial Ca_{local} and reduces the amplitude of the initial EPSC, but if enough calcium enters and binds to the buffer, it reduces its ability to buffer calcium. As a result, the second stimulus produces larger Ca_{local} than the first, and the EPSC is facilitated. **c**, A second possible mechanism is that more calcium enters for the second stimulus, and as a result there is more neurotransmitter release. This could arise from a spike broadening, or from the modulation of calcium channels. It is possible that influx through all calcium channels in the presynaptic terminal would be increased, in which case both Ca_{res} and Ca_{local} would be increased. It is also possible that the only calcium channels that are modulated are the subset that produce Ca_{local} that triggers release, in which case Ca_{res} would not be significantly increased. **d**, Finally, it is possible that there is a specialized calcium sensor that produces facilitation that is distinct from Syt1 (refs 2, 4, 45). Previous studies have shown that such a sensor would need to be sensitive to Ca_{res} based on the observation that facilitation is altered at some synapses by manipulations that affect Ca_{res} without affecting Ca_{local} . According to this scheme, release is mediated by Syt1 but calcium binding to a second sensor would increase p . The sensor is sufficiently slow that it does not influence release evoked by the first stimulus, but it is able to influence release evoked by a second stimulus.



Extended Data Figure 2 | Immunohistochemistry of Syt7 expression at four different synapses. **a–d,** Fluorescent images of immunostaining for vGlut1 (top) and syt7 (bottom) in slices from wild-type and Syt7-knockout animals, showing the stratum radiatum (SR) of hippocampal CA1 region (a), the ventral thalamus (b), mossy fibres (MF) in hippocampal CA3 (c), and the lateral and medial perforant paths (LPP and MPP) in the outer molecular layer of the dentate gyrus (d). Notably, Syt7 expression in wild-type animals was higher in the LPP, where synapses exhibit facilitation, than in the MPP, where synapses exhibit depression. Scale bar, 50 μ m. The presence of Syt7 labelling in regions containing CA3–CA1 synapses, layer 6 to thalamus synapses, mossy fibres synapses and LPP–granule-cell synapses that are also colabelled with antibodies to the presynaptic marker for glutamatergic synapses vGlut1, suggests that Syt7 is located presynaptically at these synapses. It is, however, difficult to obtain sufficient resolution with confocal microscopy in brain slices to unambiguously establish that Syt7 is located presynaptically at these synapses. Importantly, the Allen Brain atlas (<http://www.brain-map.org>) suggests that the presynaptic cells for these synapses contain messenger RNA for Syt7. Lastly, immunoelectron microscopy revealed selective staining of presynaptic boutons in the CA1 region of the hippocampus¹⁶.

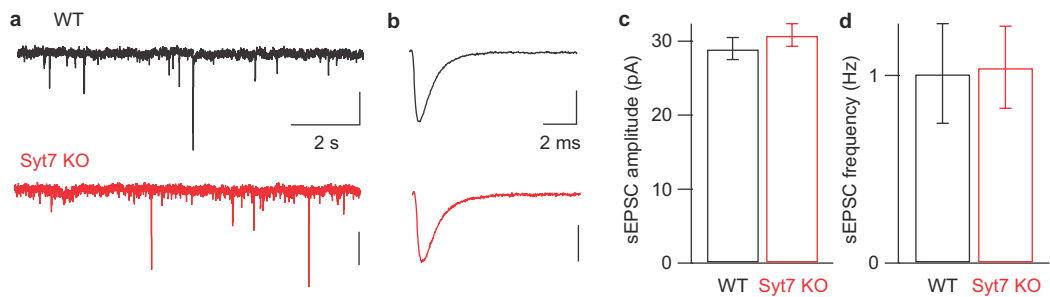


Extended Data Figure 3 | Immunohistochemistry of Syt7 and calbindin expression at mossy fibre synapses. Fluorescent images of immunostaining for calbindin-D28k, which predominantly labels mossy fibres in the CA3 region of the hippocampus^{5,46} (top) and Syt7 (bottom) in slices from wild-type and Syt7-knockout animals. Colocalization of Syt7 and calbindin staining in wild-type animals provides further support for the expression of Syt7 in mossy fibre terminals. Scale bar, 20 μm.



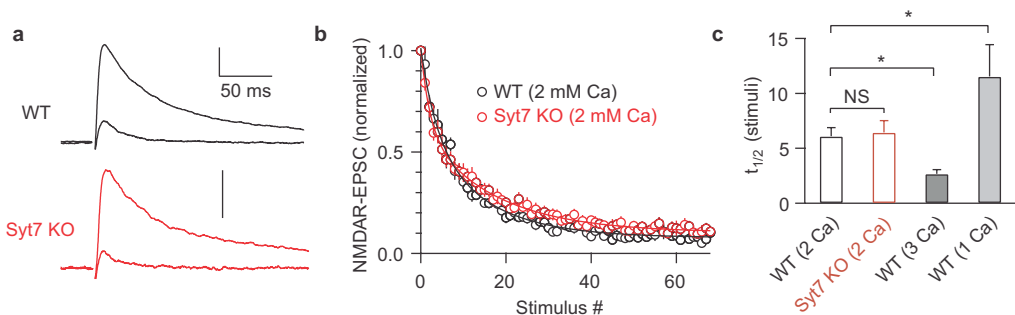
Extended Data Figure 4 | Loss of facilitation in Syt7-knockout animals at multiple frequencies. Average normalized synaptic responses evoked by extracellular stimulation with trains at frequencies from 5 to 50 Hz at four synapses in slices from wild-type and Syt7-knockout animals. Enhancement during trains was eliminated for all synapses other than mossy fibre synapses, where significant enhancement was present by the fifth stimulus for 5 Hz and 10 Hz, the third stimulus for 20 Hz, and the

sixth stimulus for 50 Hz (compared to 1 by a Wilcoxon signed rank test, $P < 0.05$). This indicates that another form of synaptic enhancement gradually builds during repetitive activation and is consistent with a specialized form of synaptic enhancement that has been described at mossy fibre synapses in which spike broadening gradually builds during repetitive activation and leads to increased calcium influx. The numbers of experiments are shown in Extended Data Table 1.



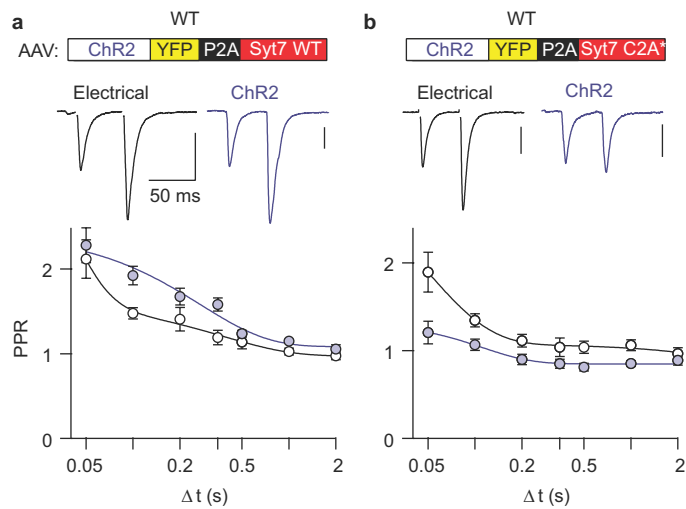
Extended Data Figure 5 | Spontaneous release is similar in wild-type and Syt7-knockout animals. **a**, Representative spontaneous EPSCs (sEPSCs) recorded from voltage-clamped hippocampal CA1 cells in wild-type (black) and knockout (red) animals. Vertical scale bars, 20 pA.

b, Representative sEPSCs, averaged from >50 events recorded in wild-type and knockout animals. Vertical scale bars, 10 pA. **c**, **d**, Average sEPSC amplitude (**c**) and frequency (**d**) in wild-type ($n=16$) and Syt7-knockout animals ($n=18$).

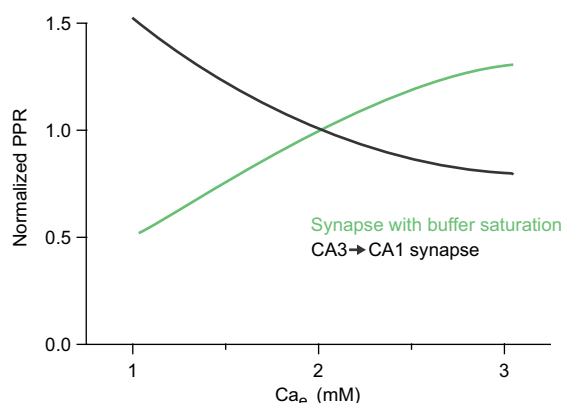


Extended Data Figure 6 | MK801 blockade of NMDAR-mediated EPSCs reveals similar initial release probability in wild-type and knockout synapses. **a**, Representative NMDAR-EPSCs recorded in wild-type and knockout animals before the application of MK801 (average of 10 traces) and after stimulation in the presence of MK801 (average response

of fifteenth to twentieth stimuli). Vertical scale bars, 100 pA. **b**, Average NMDAR-EPSCs recorded in the presence of MK801, normalized to the first stimulus. **c**, Half-decay times of NMDAR-EPSC amplitudes. $*P < 0.05$, one-way ANOVA with Tukey's post-hoc test. Data represent mean \pm s.e.m. The number of experiments is shown in Extended Data Table 2.



Extended Data Figure 7 | Effect of virally expressed Syt7 wild-type and Syt7(C2A*) in wild-type animals. **a, b,** Top, AAV was injected into the hippocampal CA3 region in wild-type animals to express ChR2 and either wild-type Syt7 (a) or Syt7(C2A*) (b). Bottom, representative EPSCs and average paired-pulse ratios for responses evoked electrically and optically in wild-type slices with AAV-driven expression of wild-type Syt7 (electrical, $n=12$; optical, $n=13$) (a) and Syt7(C2A*) (electrical, $n=5$; optical, $n=13$) (b). Vertical scale bars, 100 pA.



Extended Data Figure 8 | Evidence suggests that Syt7 does not produce facilitation by acting as a local calcium buffer at the CA3–CA1 synapse. This graph illustrates the general relationship between PPR and external calcium for synapses in which buffer saturation produces facilitation (green) and for facilitation observed at the CA3–CA1 synapse and many other synapses (black)⁹. It has been shown previously that for buffer saturation mechanism (Extended Data Fig. 1b) the amplitude of facilitation is reduced when Ca_{influx} is reduced by lowering external calcium⁹. This can be understood by considering that this form of facilitation is thought to require sufficient Ca_{influx} to saturate the endogenous buffer, and thereby reduce its ability to buffer calcium for subsequent stimuli. If Ca_{influx} is low, then there is insufficient calcium entry to bind very much of the endogenous buffer, and little facilitation would result. In addition, as shown in Extended Data Fig. 1, for a calcium buffer to produce facilitation it would need to buffer calcium sufficiently that it would reduce initial p . We have shown, however, that p is unaltered in Syt7 knockouts. This is perhaps not surprising in light of the fact that Syt7 is thought to be located on the plasma membrane, and in cases where this type of facilitation has been observed it is associated with high concentrations of a fast cytosolic buffer⁹.

Extended Data Table 1 | Number of electrophysiological recordings from wild-type and Syt7-knockout animals

Figure	Synapse	Experiment	Genotype	# of Recordings	# of Animals
Figure 1a	Schaffer collateral	Paired-pulse	WT	13	6
			KO	17	5
Figure 1b	Corticothalamic	Paired-pulse	WT	23	8
			KO	23	5
Figure 1c	Hippocampal mossy fibre	Paired-pulse	WT	10	6
			KO	8	4
Figure 1d	Lateral perforant path	Paired-pulse	WT	6	3
			KO	13	3
Figure 1e, Extended Data Figure 4	Schaffer collateral	Trains (2-50 Hz)	WT	14	6
		Trains (2-50 Hz)	KO	17	5
Figure 1f, Extended Data Figure 4	Corticothalamic	Trains (2-50 Hz)	WT	16	8
		Train (2 Hz)	KO	5	2
Figure 1g, Extended Data Figure 4	Hippocampal mossy fibre	Trains (5-50 Hz)	KO	12	3
		Train (2 Hz)	WT	3	2
Figure 1h, Extended Data Figure 4	Lateral perforant path	Train (5 Hz)	WT	7	4
		Train (10-50 Hz)	WT	10	5
		Train (2-5 Hz)	KO	3	2
		Train (10-50 Hz)	KO	8	4
		Train (2-10 Hz)	WT	3	2
		Train (20-50 Hz)	WT	6	3
		Train (2-5 Hz)	KO	5	2
		Train (10 Hz)	KO	10	3
		Train (20-50 Hz)	KO	13	3

Extended Data Table 2 | Number of experiments related to the Ca^{2+} -dependence of probability of release

Figure	Experiment	Condition	Genotype	# of Recordings	# of Animals
Figure 2a,b	Presynaptic Ca^{2+} imaging	Magnesium Green	WT	11	2
			KO	10	2
Figure 2c	Presynaptic Ca^{2+} imaging	Fura-2	WT	14	3
			KO	10	2
Figure 2d-f	Ca^{2+} -dependence of CA3-CA1 EPSC	0.5 mM Ca	WT	12	5
		1 mM Ca	WT	9	4
		2 mM Ca *	WT	15	6
		3 mM Ca	WT	6	2
		0.5 mM Ca	KO	8	4
		1 mM Ca	KO	7	6
		2 mM Ca *	KO	10	8
		3 mM Ca	KO	4	2
		20-100 uA stimulation	WT	44	11
			KO	25	8
Figure 3c,d	Ca^{2+} -dependence of CA3-CA1 fEPSP	0.5 mM Ca	WT	4	2
		1 mM Ca	WT	11	5
		2 mM Ca *	WT	11	5
		3 mM Ca	WT	8	3
		0.5 mM Ca	KO	4	4
		1 mM Ca	KO	8	4
		2 mM Ca *	KO	9	5
		3 mM Ca	KO	6	3
Figure 3e-g	MK801 blockade of NMDAR-fEPSP	2 mM Ca, single stim	WT	6	2
		2 mM Ca, triple stim	WT	5	3
		2 mM Ca, single stim	KO	6	3
		2 mM Ca, triple stim	KO	4	3
Extended Data Figure 6	MK801 blockade of NMDAR-EPSC	1 mM Ca	WT	14	3
		2 mM Ca	WT	11	4
		3 mM Ca	WT	3	2
		2 mM Ca	KO	9	4

*To normalize responses in different Ca^{2+} concentrations, all Ca^{2+} -dependence experiments included recordings in 2 mM Ca^{2+} followed by wash in of different Ca^{2+} concentrations.